Temporal proteomic profiling reveals insight into critical developmental processes and temperature-influenced physiological response differences in a bivalve mollusc

Shelly A. Trigg[1]*, Kaitlyn R. Mitchell[1], Rhonda Elliot Thompson[1], Benoit Eudeline[2], Brent Vadopalas[3], Emma B. Timmins-Schiffman[4], and Steven B. Roberts[1]

[1]School of Aquatic and Fishery Sciences, University of Washington, Seattle, Washington, USA

[2]Taylor Shellfish Hatchery, Quilcene, Washington, USA

[3]Washington Sea Grant, University of Washington, Seattle, Washington, USA

[4]Department of Genome Sciences, University of Washington, Seattle, Washington, USA

***Corresponding author:**
Shelly A. Trigg
strigg@uw.edu
School of Aquatic and Fishery Sciences
University of Washington
Seattle, WA 98105

ABSTRACT

Protein expression patterns underlie physiological processes and phenotypic differences including those occurring during early development. The Pacific oyster (*Crassostrea gigas*) is particularly fascinating as it undergoes a dramatic transformation from free-swimming larval form to sessile benthic dweller, and proliferates in environments widely ranging in temperature. Here, we comprehensively characterized protein expression patterns for 7978 proteins throughout metamorphosis in the Pacific oyster at two temperature regimes to gain a better understanding of how developmental processes are altered. We used a multi-statistical approach including principal component analysis, ANOVA-simultaneous component analysis, and hierarchical clustering coupled with functional enrichment analysis to characterize these data. We identified distinct sets of proteins with time-dependent abundances generally not affected by temperature. Over time, adhesion and calcification related proteins acutely decreased, organogenesis and extracellular matrix related proteins gradually decreased, proteins related to signalling showed sinusoidal abundance patterns, and proteins related to metabolic and growth processes gradually increased. Contrastingly, different sets of proteins showed temperature-dependent abundance patterns with proteins related to immune response showing lower abundance and catabolic pro-growth processes showing higher abundance in animals reared at 29°C relative to 23°C. These abundance pattern differences correspond to larger oyster size observed at the elevated temperature and are likely indicative of a combination of differences in specific metamorphic processes and possible pathogen presence. The proteome resource generated by this study provides data-driven guidance for future work on developmental changes in molluscs. Furthermore, the analytical approach taken here provides a foundation for effective shotgun proteomic analyses across a variety of taxa.

Keywords

Proteomics, time-series, developmental physiology, oyster, temperature, mollusc

INTRODUCTION

The Pacific oyster (*Crassostrea gigas*) is among the most prominent molluscs given its contribution to biofiltration, habitat formation and stabilization, carbon and nitrogen sequestration, and international aquaculture revenue. From a developmental perspective, it is a fascinating organism as it undergoes a complex transformation from a free-swimming planktonic larva to a sessile benthic juvenile. This involves two processes: settlement and metamorphosis. Once oysters acquire the ability to initiate and undergo morphogenesis (become competent), settlement commences typically 24 to 48 hours later where larvae drop out of the water column to the benthos, and use a newly developed foot to find appropriate substrate and secrete adhesive to attach to the substrate (Foulon et al. 2019; Coon et al. 1990). Then, metamorphosis typically occurs within a few to 72 hours and involves a complete rearrangement of organs, loss of larval organs including the velum and the foot, and development of new organs including gill-like ctenidia (Plough 2018; Baker and Mann 1994). Complex physiology underlies both of these processes, involving neuroendocrine and immune functions and tightly-controlled gene expression programs, which is still not fully understood (Joyce and Vogeler 2018).

In addition to the physiological complexities of settlement and metamorphosis, Pacific oyster are particularly sensitive to abiotic and biotic factors during this life stage with substantial mortality occurring in both field and culture settings (Plough 2018). Past studies found that increased rearing temperature positively influenced survival with Pacific oyster larvae reared at 23°C leading to optimal recruitment success (Quayle 1988; Korringa 1976; Kobayashi et al. 1997), and established 23°C as the standard aquaculture industry rearing temperature (Helm and Bourne 2004). Yet hatcheries still frequently observe stochastic high mortality during this life stage. More recent studies demonstrated that further increasing the rearing temperature to 27-29°C significantly improves survival during settlement (Rico-Villa et al. 2009; His et al. 1989; Helm and Millican 1977; G Crandall, R Elliot Thompson, B Euladiene, B Vadopalas, EB Timmins-Schiffman, & SB Roberts, *unpublished*). To better understand how temperature

influences critical developmental processes and phenotype throughout metamorphosis, a comprehensive characterization of developmental physiological processes that occur throughout this life stage is needed.

Proteomics, a survey of the collection of all proteins and their abundances at a given time, is ideally suited to provide a basis for revealing the physiological complexities of development (Casas-Vila et al. 2017). Specifically, untargeted shotgun proteomic profiling using liquid chromatography coupled tandem mass spectrometry (LC-MS/MS) can efficiently and accurately predict protein abundances by taking into account peptide count, spectral count and fragment-ion intensity (Griffin et al. 2010). LC-MS/MS has been effectively used to examine changes in biological processes during early Pacific oyster larval development prior to metamorphosis (Dineshram et al. 2016; Huan et al. 2012). One study did a two sample proteomic comparison of larvae just prior to metamorphosis with juveniles weeks after metamorphosis, however the two proteomes had relatively low coverage (392 and 636 proteins, respectively) (Huan et al. 2015). Deeper proteomic profiling of a broader sampling throughout metamorphosis and including temperature as a factor would bring more resolution to physiological processes occurring over time and those affected by temperature. Although untargeted large-scale multi-factor proteome studies pose the challenge of identifying core biological responses in the accompanying large complex datasets, applying multiple statistical approaches can reduce complexity of a large dataset to identify potential targets for diagnostics (Grissa et al. 2016; Trigg, et al. 2019). New analyses have been developed to consider temporal influences on multivariate datasets (e.g. analysis of variance simultaneous component analysis (ASCA)), and identify features impacted by specific experimental variables (Smilde et al. 2005).

To comprehensively characterize developmental physiological processes that occur throughout settlement and metamorphosis in the Pacific oyster, we used LC-MS/MS to generate temporal proteomes from oyster larvae reared two different temperature regimes to examine the basis for temperature-influenced phenotype differences. We developed an analysis framework that applies multiple

statistics to classify temporal and temperature-influenced developmental processes from proteomic responses. This longitudinal proteomic dataset and associated phenotype data offer greater clarity on biological processes underlying specific metamorphic stages and how temperature influences these processes.

RESULTS

Larval performance and global proteome analysis

To comprehensively assess proteomes throughout metamorphosis we collected pools of whole animals at seven different time points starting at competency, the time when larvae have the ability to initiate and undergo metamorphosis (**Figure 1A**). We found no difference in larval survival or settlement among those reared at 23°C and those reared at 29°C, however larvae reared at 29°C tended to be larger in size at 24 days post-fertilization (dpf), 6 days into temperature treatment (**Figure 1B**, **Supplemental Table 1**).

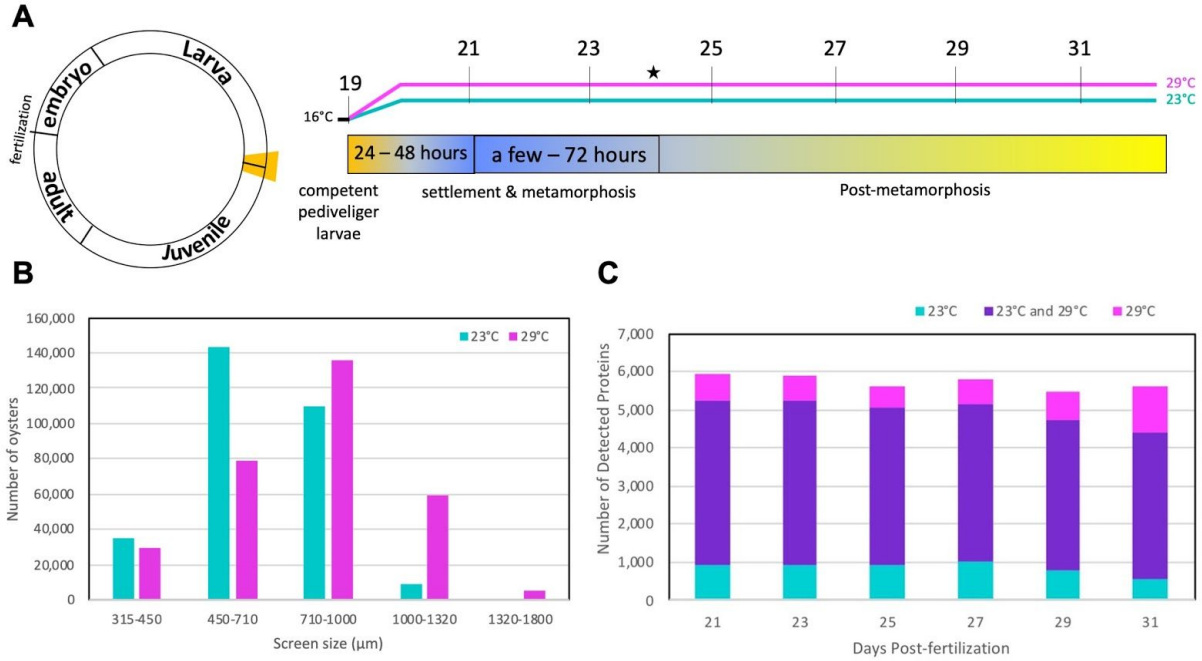

Figure 1. Pacific oyster developmental proteome during metamorphosis. (**A**) Diagram depicting life cycle period examined and the collected time points in days post fertilization at each temperature regime. Color bar shows typical timing of metamorphic transitions. The time point when settlement was assessed is denoted by a star. (**B**) Size

distribution based on sorting screen size of oysters at 24 days post-fertilization when settlement was assessed. (**C**) Number of detected proteins at each time point across two rearing temperatures (23°C, cyan; 29°C, magenta, present in both, purple).

Quantitative time-series proteomic measurements collectively yielded 7978 proteins, with proteomes at each time point having an average of 4936 ± 255 (s.d.) proteins. Technical replicates from the same time point clustered together and showed less variability than samples from different time points, demonstrating the high reproducibility of our sample preparation and LCMS/MS measurements (**Supplemental Figure 1**). There was an average overlap of 84 ± 3% of proteins identified in samples from the same time point but different rearing temperature (**Figure 1C**, **Supplemental Table 2**). A principal components analysis revealed temperature most strongly influenced protein abundance patterns at 21 and 27 dpf, while at 23, 25, 29, and 31 dpf temperature had less of an influence (**Figure 2A)**. From this analysis a total of 70 proteins were identified as top contributors to this temperature-influenced proteomic variation at 21 and 27 dpf, and showed three general abundance patterns: decreased abundance at 29°C relative to 23°C at 21 dpf (pale yellow clade), decreased abundance at 29°C relative to 23°C at 27 dpf (salmon clade), and increased abundance at 29°C relative to 23°C at 27 dpf (pale purple clade) (**Figure 2B**, **Supplemental Table 3**). Proteins with decreased abundance at 29°C relative to 23°C at 21 dpf show significant enrichment of cytoskeleton and extracellular matrix organization, cell motility and locomotion processes (**Figure 2C**). Proteins with decreased abundance at 29°C relative to 23°C at 27 dpf have significant enrichment of early stage development as well as stress response, transport, and catabolic processes, while proteins with increased abundance at 29°C relative to 23°C at 27 dpf have significant enrichment of cellular component and protein complex assembly, transport, and immune system processes. (**Figure 2C**).

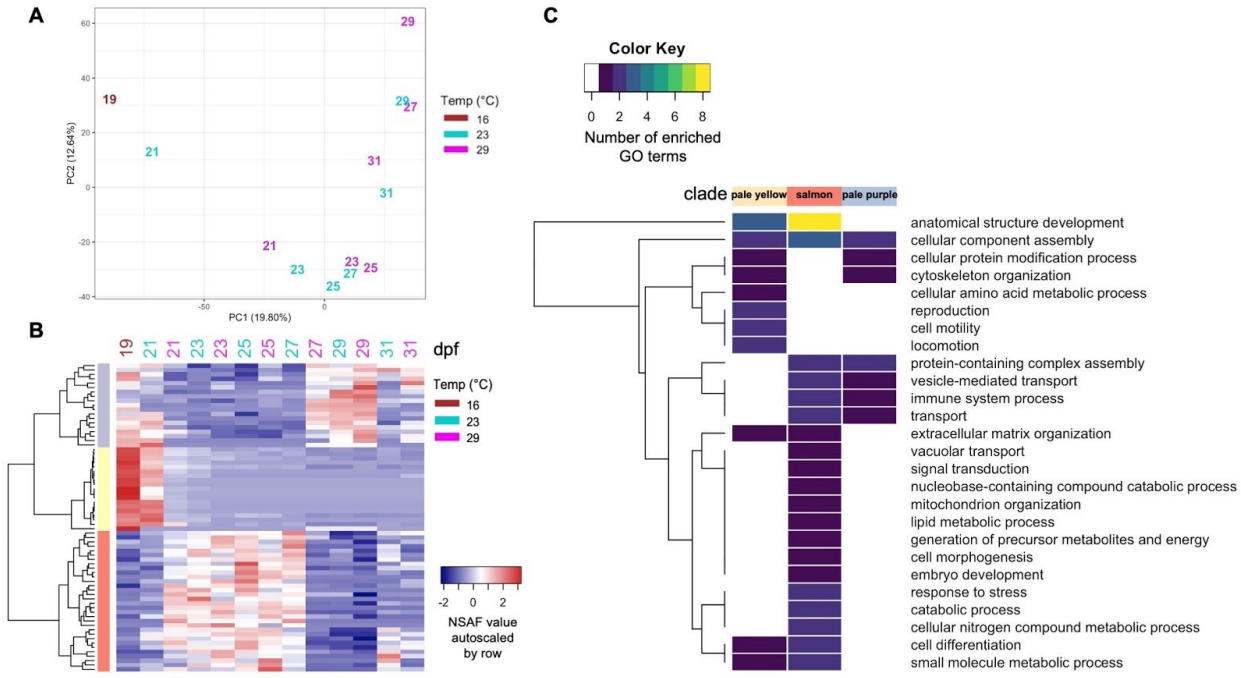

Figure 2. Temperature most influences 21 and 27 dpf proteomes. (**A**) Visualization of the first two principal components from principal component analysis separating samples according to their developmental stage and temperature. Samples are labeled by their sampling time point in days post-fertilization (dpf) with color indicating rearing temperature (16°C, brown; 23°C, cyan; 29°C, magenta). (**B**) Protein abundances (NSAF values autoscaled by row) of proteins most influenced by temperature at 21 and 27 dpf. (**C**) Summary of biological processes represented by enriched GO terms within each clade for temperature-influenced proteins at 21 and 27 dpf.

Time-influenced proteomic variation

An ANOVA-simultaneous component analysis (ASCA) that partitioned effects from time, temperature, and their interaction revealed that time and the interaction of time and temperature contributed 91.38% to the variation in protein abundances (**Table 1**). However, a permutation test to quantitatively validate ASCA megavariate effects (Zwanenburg et al. 2011) showed that only time had a significant effect on protein abundances (**Table 1**). A total of 217 proteins contributed the most to abundance pattern differences across time (**Figure 3A**). Five distinctive clades were identified through cluster analysis of abundance patterns of these time-influenced proteins (**Figure 3B)**. The identified clades exhibit temporal patterns that appear generally independent of temperature: high abundance early on then acutely reduced (light blue clade), a gradual decrease in abundance over time (purple clade),

oscillating abundance that increases through 25 dpf then decreases through 29 dpf and finally increases again at 31dpf (green clade), oscillating abundance that decreases through 25 dpf then increases through 29 dpf and finally decreases at 31dpf (gray clade), and a gradual increase in abundance over time (black clade) (**Figure 3C**) .

Table 1. Contributions of experimental factors to the ASCA-partitioned data variation and permutation validation test results.

Factor	Variation (%)	Permutation test (*P* value)
Time	56.85	0.0026
Temperature	8.56	0.1882
Time:Temperature	34.59	0.9981

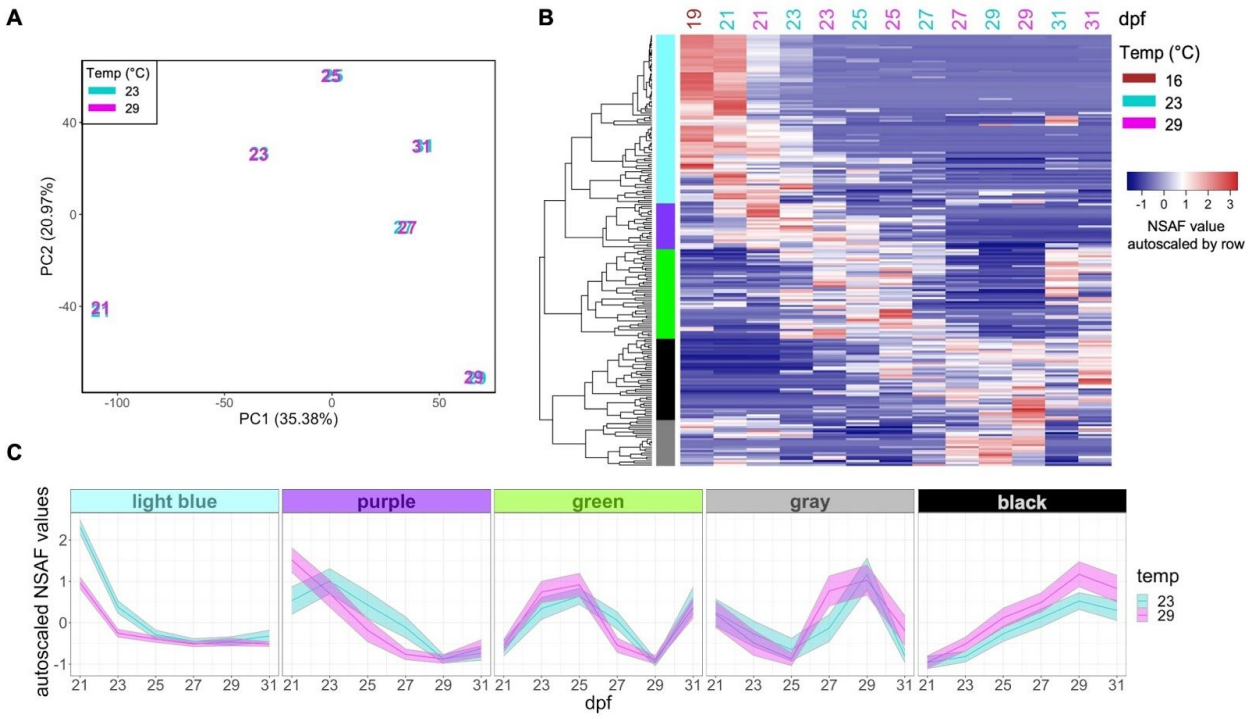

Figure 3. Influence of time on proteomes. (**A**) Simultaneous component analysis of variation influenced by time, samples are labeled by their sampling time point in days post-fertilization (dpf) with color indicating rearing temperature (23°C, cyan; 29°C, magenta). (**B**) Protein abundances (NSAF values autoscaled by row) of 217 proteins that contributed the most to time-influenced proteomic variation. (**C**) Temporal abundance patterns of 217 time-influenced proteins based on 5 clades. Bolded line, autoscaled NSAF clade mean with 95% confidence intervals shown.

Biological processes associated with anatomical structure development and cell differentiation were commonly enriched among proteins across most clades, however, there was a distinct set of enriched biological processes for each clade suggesting specific functions for proteins within each clade (**Figure 4**, **Supplemental Table 4**). Proteins showing high abundance early on then an acute decrease (light blue clade) were related to immune system, stress response, cell proliferation, cell adhesion, nucleocytoplasmic transport, and cellular amino acid metabolism. Proteins showing a gradual decrease in abundance over time (purple clade) were related to cellular component assembly and protein complex assembly processes. Proteins with oscillating abundance that first increases, then decreases, then increases again (green clade) were related to protein modification, stress response, signal transduction, cell death, and transport biological processes. Different than other clades, this clade had more enriched GO terms related to lipid metabolic process, cell death, cellular amino acid metabolic process, locomotion, and cell motility. Proteins with oscillating abundance that first decreases, then increases, then decreases again (gray clade) were associated with cytoskeleton organization, transport (protein localization, lysozyme transport), and morphogenesis. Different than other clades, this clade had more enriched GO terms related to transport (vesicle transport, vacuolar transport), cell-cell signaling, cytoskeleton organization, protein maturation and developmental maturation. Proteins showing a gradual increase over time (black clade) were largely related to growth and development processes, particularly energy-generating glycolytic processes (e.g. fructose metabolism, mannose metabolism, oligosaccharide metabolism, ganglioside catabolism, and adenosine catabolism) and neurogenesis. These proteins had significant enrichment of GO terms related to carbohydrate metabolic process, cofactor metabolic process, generation of precursor metabolites and energy, nervous system process, plasma membrane organization, and nucleobase-containing compound catabolic process.

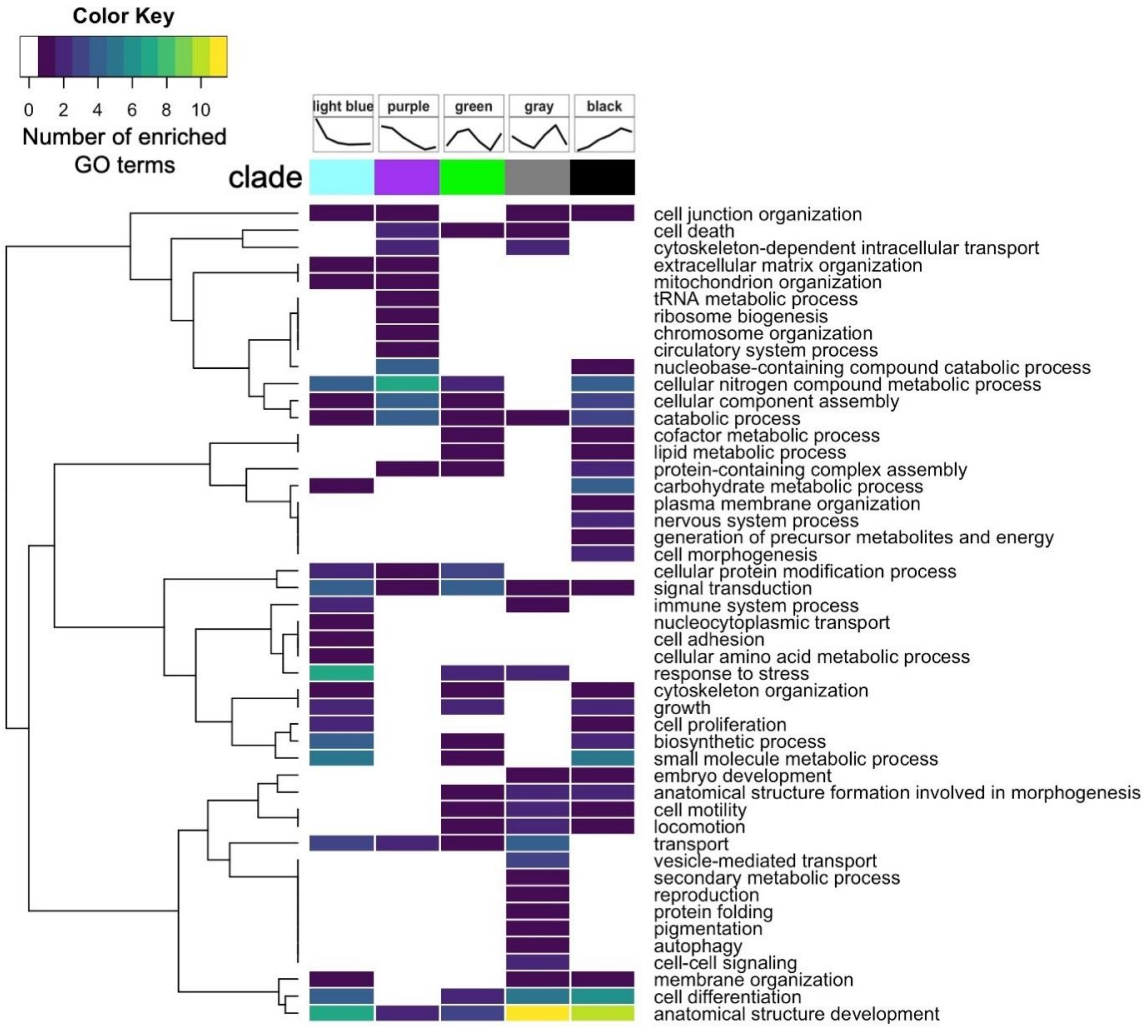

Figure 4. Summary of biological processes represented by enriched gene ontology terms within each clade for time-influenced proteins.

Proteome response to temperature

Although the ASCA-partitioned effect of temperature was not validated as significant by permutation test (**Table 1**), we still explored proteins contributing to the ASCA-modeled separation of samples by temperature (PC1, **Figure 5A**). We found 259 proteins to be significantly influenced by temperature and hierarchical clustering of these patterns revealed two distinctive clades that generally show increased or decreased abundance in 29°C relative to 23°C samples throughout time (orange clade and dark teal clade, respectively; **Figure 5B-C**, **Supplemental Table 5)**. Proteins showing increased

abundance in 29°C relative to 23°C (orange clade) were enriched for growth and development related processes while proteins showing decreased abundance in 29°C relative to 23°C (dark teal clade) were enriched for transport, catabolism, and immune system related processes (**Figure 6**). Immune related proteins in the dark teal clade include putative RNA helicase DEAD box proteins 47 and 58 known to be involved in cellular response to exogenous dsRNA and a putative exosome complex component protein involved in RNA degradation; two homologs of Heme-binding protein 2 and a putative Receptor-interacting serine/threonine-protein kinase 1 known to be involved in positive regulation of necrotic cell death; a putative DnaJ Heat Shock Protein Family (Hsp40) Member A3 known to be involved in cell death activation and growth inhibition; a putative cytidine deaminase known to be involved in signalling and growth inhibition; and a putative COMMD9 involved in neutrophil degranulation.

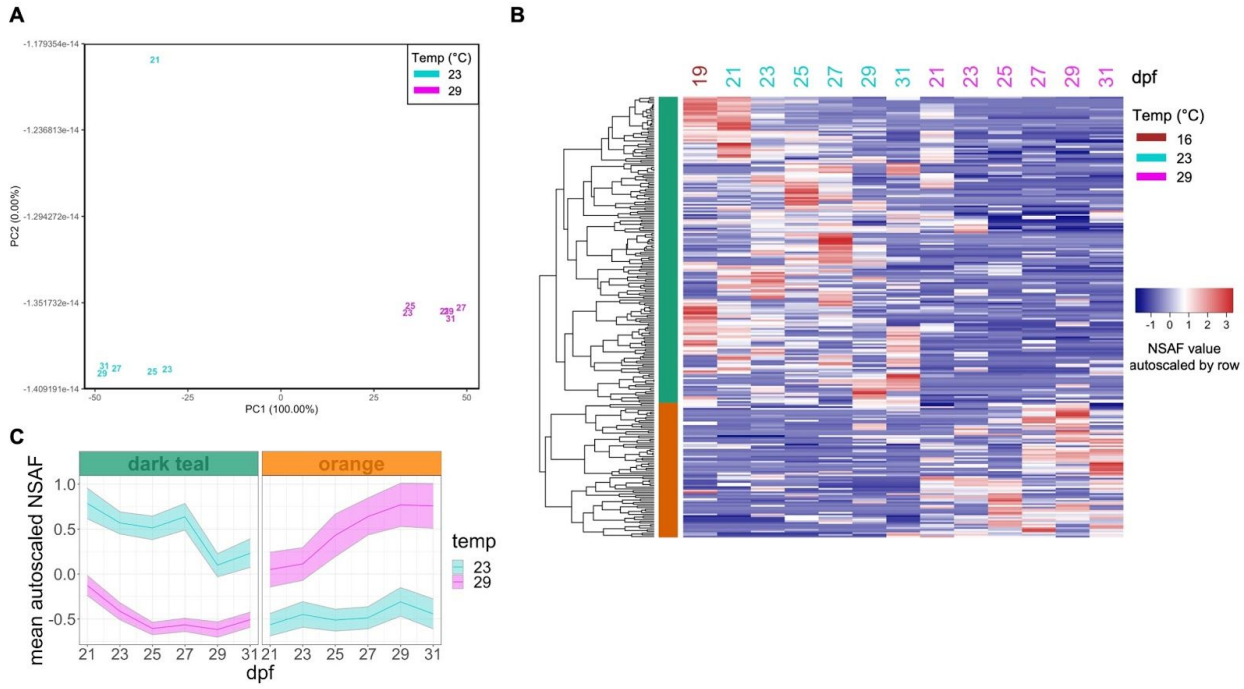

Figure 5. Temperature influence on proteomes. (**A**) Simultaneous component analysis of variation influenced by temperature, samples are labeled by their sampling time point in days post-fertilization (dpf) with color indicating rearing temperature (23°C, cyan; 29°C, magenta). (**B**) Protein abundances (NSAF values autoscaled by row) of 259 proteins that contributed the most to temperature-influenced proteomic variation. (**C**) Temporal abundance patterns of 259 temperature-influenced proteins based on 2 clades. Bolded line, autoscaled NSAF clade mean with 95% confidence intervals shown.

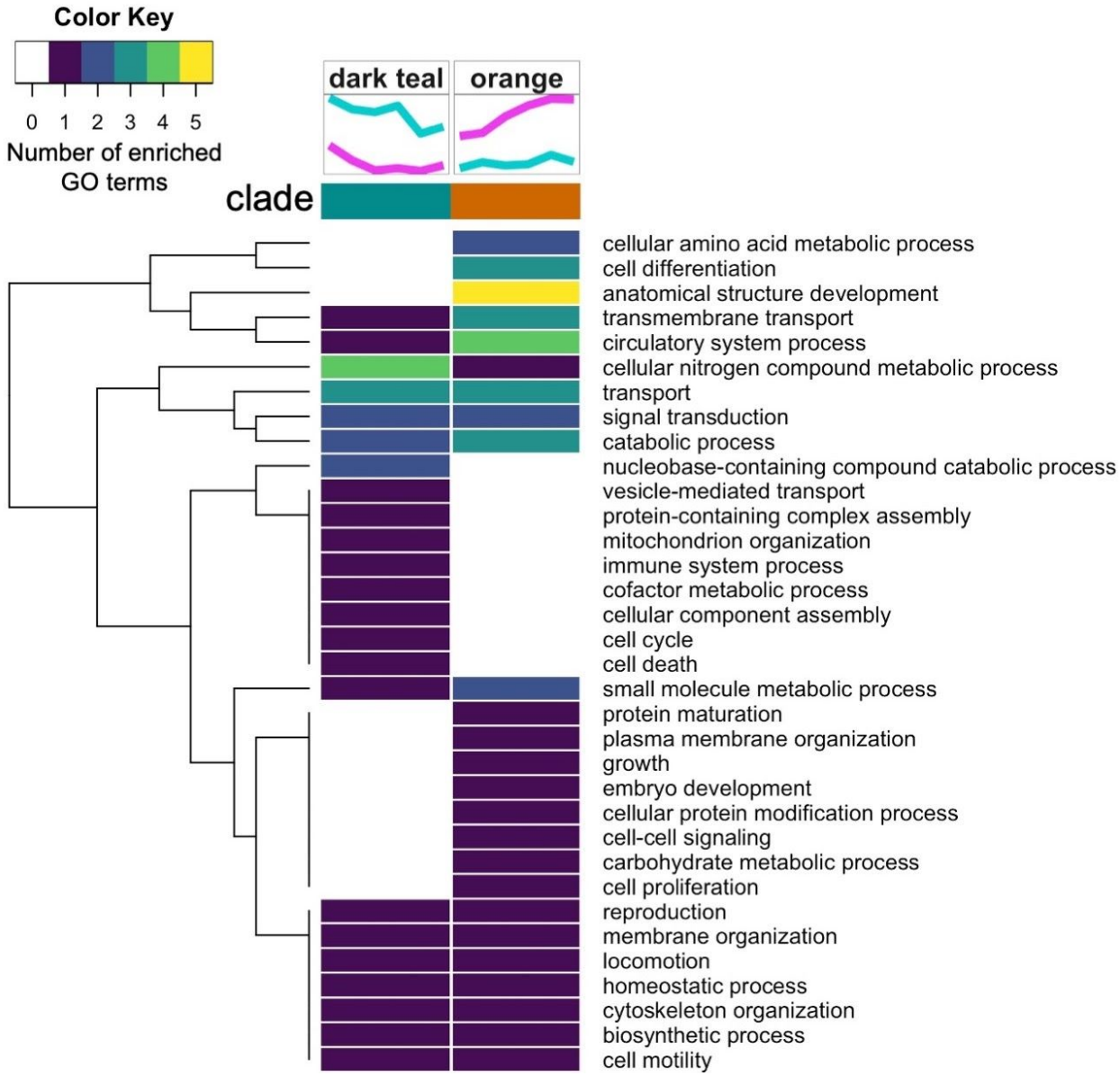

Figure 6. Summary of biological processes represented by enriched GO terms within each clade for temperature-influenced proteins.

DISCUSSION

We used time series proteomics to explore how oyster physiology is affected by rearing temperature during metamorphosis, generated comprehensive proteomes at seven different time points with six across two different temperatures, and did a comparative analysis of how time and temperature affect proteins and their associated biological processes. Performing ASCA, a method which generalizes

analysis of variance to a multivariate case (Smilde et al. 2005), allowed the variation in the proteomic data to be partitioned by the experimental factors of temperature, time and their interaction. From this partitioning, we were able to identify proteins that most contribute to variation across time points and variation between temperatures. We were able to further classify differentially abundant proteins by performing hierarchical clustering of their abundance patterns and assigning clades to distinct patterns of abundance change over time and across temperatures. This multi-statistical approach led to the identification of proteins with time and temperature-dependent abundance patterns (**Figures 3** and **5**), and while we could have been more precise in thresholding PC loadings to select proteins, we chose to be more inclusive as to not limit the scope of this exploratory study. Although time and the interaction of time and temperature explained more of the ASCA-partitioned variation in the proteomes, a permutation validation test revealed time had the greatest effect on protein abundance, followed by temperature, and lastly by the interaction of time and temperature (**Table 1**). We chose to not examine the time:temperature interaction effect because the permutation validation test suggested our observations were not different than random chance. However, we chose to examine the temperature effect because it was nearer to being significant and examining proteins contributing to ASCA-partitioned temperature variation allowed two distinct temperature-dependent abundance patterns to emerge. Through examining proteins contributing to time and temperature variance we were able to provide comprehensive insight into the proteomic landscape throughout oyster development in conjunction with the nuanced influence of temperature.

We found that temperature only moderately affected proteomes similar to previous findings (Dineshram et al. 2016), and that time was a stronger driver of proteomic differences across samples. This is consistent with the concept that gene expression patterns enable underlying physiological programs to be preserved in order for oysters to achieve key developmental stages in different environmental conditions (Meistertzheim et al. 2007; Dineshram et al. 2016; Ginger et al. 2013). The five distinct protein

abundance trends over time are suggestive of particular developmental processes persisting and remaining in sync despite temperature differences.

During typical development, swimming pediveliger larvae settle around 18 dpf, and within 1 to 3 days after settlement most larvae complete metamorphosis to the juvenile stage (Baker and Mann 1994). In our experiment, two days after larvae appeared competent at 21 dpf, proteins that had high abundance and were then acutely reduced over time (light blue clade) aligned with larval settlement. Seven of the 42 proteins with Uniprot annotations in this clade, and no proteins from other clades, previously showed pediveliger stage-specific expression (CGI_10004853, CGI_10010615, CGI_10006921, CGI_10026725, CGI_10010375, CGI_10006922, and CGI_10006919) (Foulon et al. 2019). Among other light blue clade proteins were three protease inhibitors, nine structural proteins mostly related to collagen, and five calcification-related proteins that did not previously show pediveliger stage-specific transcript expression, but support hypotheses previously formulated about adhesion during larval settlement (Foulon et al. 2019). These differences between transcript and protein abundances during settlement highlight the importance of proteomics studies to complement transcriptomics studies.

A key feature of metamorphosis following pediveliger settlement is organ revolution in an anterior-dorsal direction (Baker and Mann 1994). Proteins that had high abundance at 23 dpf followed by a gradual decrease over time (purple clade) showed clade-specific enrichment of processes related to cell component assembly and protein complex assembly. These included structural proteins (dynein 2 light chain and laminin B2), cell fate determining proproteins (ADAM-TS 16, ADAM-TS 17, and Notch3), and a protein catabolism promoting protein (Cell death regulatory protein GRIM-19), all of which support a tight regulation of growth, cell differentiation and movement that could underlie organ rearrangement at this time point. Moreover, the exosome complex component protein (RRP40) related to the clade-specific enrichment of nucleobase-containing compound catabolism, tRNA metabolic and ribosome biogenesis

related processes may play a role in modulating the abundance of pediveliger-specific and recently metamorphosed juvenile-specific lincRNAs (Yu et al. 2016).

As metamorphosis consists of both degradation (e.g. velum and foot degradation) and growth processes (e.g. gill and adductor muscle development), it is intriguing how these two opposing processes might occur around the same time. Interestingly, we observed two opposing trends in protein abundance patterns over time that were generally unaffected by temperature. Proteins with abundances that increase through 25 dpf then decrease through 29 dpf and increase again at 31dpf (green clade) showing clade-specific enrichment of protein modification and signal transduction related processes are generally related to growth promoting pathways. For instance green clade proteins Map kinase kinase 4, Map kinase kinase 5, and PAK-1 are all members of the MAPK signalling pathway that activates cell differentiation and proliferation, potentially related to the development of gill tissue during the prodissoconch and dissoconch postlarval stages and the development of the adductor muscle in the early juvenile stage (Baker and Mann 1994). Additionally, proteins underlying clade-specific enrichment of lipid and cofactor metabolic processes include oxidative stress protective enzymes paraoxonase and glucose-6-phosphate dehydrogenase which likely act to counter the reactive oxygen species resulting from the aerobic respiration that metamorphosis requires (Baker and Mann 1994). Proteins with abundances showing an opposing trend decreasing through 25 dpf, then increasing through 29 dpf and decreasing again at 31dpf (gray clade) had clade-specific enrichment of cell-cell signaling and transport processes. These included a protein involved in neurotransmitter release regulation (Snapin), GABA type A receptor-associated protein, Hsc70-interacting protein, and a number of cytoskeleton related proteins (Rho1, Tubulin-folding cofactor B, Filamin-B, and muscle actin LpM) involved in growth regulation. The increased abundance of these proteins at 27-29 dpf could serve in signalling the downregulation of processes initiated by the growth-related proteins at 23-25dpf (green clade). The potential growth-curbing role of the gray clade proteins is further supported by their decreased abundance at 31 dpf and the enrichment of growth

promoting and carbohydrate metabolic processes in proteins showing an increase over time peaking at 31 dpf (black clade). At this time point, the high abundance of fatty acid binding proteins (H-FABP and B-FABP), muscle growth-related proteins (Thymosin beta, Tropomyosin, and Collagen alpha-3 (VI) chain), and carbohydrate metabolic proteins (Hexokinase type 2, Fructose-bisphosphate aldolase, and Ganglioside GM2 activator) is suggestive of muscle tissue building and maintenance (e.g. adductor muscle) that occur after the establishment of structural components, and that the final juvenile stage has been reached.

Although temperature did not have as dominant an effect as time on protein abundances, the two distinct temperature-dependent protein abundance patterns and their associated biological processes support the phenotypic differences we observed in larvae reared at different temperatures. The growth and development-related processes enriched among proteins showing increased abundance in 29°C relative to 23°C regardless of time support the larger sizes observed for animals reared 29°C compared to 23°C at 24 dpf. While this could be due to elevated temperature increasing overall development rate (O'Connor et al. 2007; Filgueira et al. 2015) by increasing ingestion activity (Rico-Villa et al. 2009; Humphries 2013), we did not detect a significant time:temperature interaction effect. We did, however, observe specific time points where temperature appeared to have a greater impact on protein abundance (21 and 27 dpf). For example, proteins showing increased abundance at 21 dpf (pale yellow clade) related to motility at 23°C (e.g. cilia and flagella associated proteins 53, 54, 58, and 43, TPR repeat protein 25, and tektin-4) could indicate the persistence of the velum organ at 23°C and its degradation at 29°C. The decreased abundance of muscle forming proteins, filament proteins, and signalling proteins at 27 dpf in animals reared at 23°C (pale purple clade) suggests that muscle formation is less robust at 23°C than at 29°C. Of the 79 proteins showing increased abundance regardless of time in 29°C relative to 23°C (orange clade), 11 have previously shown increased abundance in response to various 30°C stress conditions in a proteomics

study on pediveliger (15-17 dpf) Pacific oyster (Dineshram et al. 2016) (**Table 2**). Nine of these proteins are characterized and are commonly involved in smooth muscle and neuron formation.

Table 2. Proteins that commonly show increased abundance in response to high temperature.

Protein ID	Uniprot ID	Gene ID	Protein name	Function
CHOYP_contig_043280.m.49983	K1PZS2	CGI_10005951	Uncharacterized protein	unknown
CHOYP_LOC100705966.1.1.m.45957	K1QJR4	CGI_10019738	Heat shock protein beta-1	stress resistance and actin organization (Kostenko et al. 2009), regulates transport of neurofilament proteins (Kostenko et al. 2009; Holmgren et al. 2013)
CHOYP_ADD.3.5.m.17639	K1PEX5	CGI_10006848	Protein hu-li tai shao	actin assembly, important for neuromotor function
CHOYP_LOC100367954.2.2.m.66596	K1P9U4	CGI_10005881	Uncharacterized protein	unknown
CHOYP_LOC100375029.6.10.m.36981	K1QM61	CGI_10009700	Uncharacterized protein	actin monomer binding [GO:0003785]; actin filament organization [GO:0007015]
CHOYP_LOC100375029.8.10.m.60484	K1QM61	CGI_10009700	Uncharacterized protein	actin monomer binding [GO:0003785]; actin filament organization [GO:0007015]
CHOYP_LOC101173335.4.4.m.49816	K1PFT9	CGI_10006016	Transgelin	actin cross-linking/gelling protein in fibroblast and smooth muscle tissue (Matsui et al. 2018; Thweatt et al. 1992; Assinder et al. 2009)
CHOYP_NF70.1.4.m.31159	K1PWQ2	CGI_10018067	60 kDa neurofilament protein	intermediate filament [GO:0005882]
CHOYP_RPS24.1.8.m.571	K1PUV4	CGI_10001493	40S ribosomal protein S24	ribosome [GO:0005840]; structural constituent of ribosome [GO:0003735]; translation [GO:0006412]
CHOYP_contig_044078.m.50900	K1Q086	CGI_10019530	Ankyrin-2	essential role in localization and membrane stabilization of ion transporters in muscle cells (Cunha et al. 2007; Mohler et al. 2003), signal transduction [GO:0007165]
CHOYP_LOC100696604.1.1.m.40638	K1QP17	CGI_10010975	Caprin-1	directly binds mRNA involved in neuronal synaptic plasticity, cell proliferation, and migration in multiple cell types; may regulate mRNA transport and translation (Solomon et al. 2007)

The immune system, vesicle transport, and nucleobase-containing, nitrogen compound catabolic processes associated with proteins showing decreased abundance in animals reared at 29ºC (dark teal

clade) are likely associated with metamorphic differences (e.g. different degradation rates of velum or foot), differences in metabolic rate, differences in pathogen presence, or a combination of these. For instance, viral recognition protein DEAD box protein 58 and growth inhibition/cell death-related proteins serine-threonine kinase receptor-associated protein and DNAj-like protein have been implicated in dsRNA exposure response in adult Pacific oyster gill tissue (Masood et al. 2016). Reduced abundance of these proteins in animals at 29ºC suggests they were not sustaining immune and cytoprotection processes, allowing them to reallocate energy to growth (Genard et al. 2013). Moreover, potential pathogen exposure in animals reared at 23°C could have led to a decline in feeding activity and therefore less growth (Genard et al. 2013). A delay in velum degradation in oysters reared at 23°C could have led to an immune challenge as the velum in particular has shown susceptibility to infection (Ushijima et al. 2018; Estes et al. 2004; Renault and Novoa 2004). Further controlled trials are needed to determine the extent to which these specific proteome differences are driven by a pathogenic response, metabolic rate differences, and/or specific metamorphic process differences.

In conclusion, we successfully simultaneously surveyed thousands of proteins to generate comprehensive proteomes from which we were able to identify temporal and temperature-influenced protein abundance patterns. We characterized physiological processes related to proteins with different abundance patterns that underlie core developmental processes in addition to describing the influence of different temperature regimes. The proteome resource generated provides new insight into developmental processes occurring throughout metamorphosis that can serve as hypotheses and data-driven guidance for future research on specific metamorphic stage transitions, better understanding temperature-related phenotypic differences in mollusc development, and developmental regulation in general. Lastly, the analytical approach taken here provides a foundation for effective shotgun proteomic analyses across a variety of taxa.

METHODS

Larval rearing

All seawater used for rearing flowed continuously from Dabob Bay, WA at 3 L/min, filtered to 5µm, and was maintained at pH 8.4 by the addition of sodium carbonate. Animals were fed T-*Isochrysis*, *Pavlova* sp., *Nannochloropsis* sp., *Rhodomonas* sp., and *Tetraselmis* sp. at constant effluent algal densities of 100,000 cells/mL throughout the experiment. *Crassostrea gigas* (triploid) larvae were reared at 16°C until they developed eyespots and pedal appendages, and were greater than 250 µm in size (pediveliger stage; 19 days post-fertilization). An initial sample of ~12,500 pediveliger larvae was rinsed with filtered seawater, dried, flash frozen in liquid nitrogen and stored at -80ºC for proteomics analysis. Approximately one million pediveligers (20.0 g) were transferred to the experimental rearing system consisting of a silo (46 cm PVC pipe) containing 80mL of ground oyster shell (180-315 µm graded microculch) as settlement substrate. Each silo was housed inside a rearing tank with flowing filtered seawater and held at either 23°C or 29°C for 13 days. Tanks were drained and oysters were rinsed with filtered seawater daily.

Settlement assessment and sampling

At 24 days post-fertilization, settlement and size were assessed using sorting screens ranging from 450 to 1320 µm, and any larvae that had not set were removed. Settlement was calculated as the proportion of larvae captured on the sorting screens. At 21, 23, 25, 27, 29, and 31 days post-fertilization (corresponding to days 3, 5, 7, 9, 11, and 13 of the experiment, respectively) samples of approximately 12,500 larvae were collected from each of the two temperature regimes (23°C or 29°C) for shotgun proteomics analysis. Larvae were rinsed with filtered seawater, dried, flash frozen in liquid nitrogen and stored at -80°C. In total there were 13 samples taken for proteomic analysis, one initial sample from 19 days post-fertilization at 16°C and six at each temperature regime throughout development.

Protein Sample Preparation

Cell homogenates were prepared by adding 500 µL of 50 mM NH_4HCO_3 in 6 M urea to the sample and homogenizing with a pestle directly in the microfuge tube. Samples were centrifuged at 2000 rpm for 5 minutes and supernatant (150 µL) was transferred into new tubes. Supernatants were sonicated three times each for 5 seconds, cooling samples in between sonication rounds using an ethanol and dry ice bath for 5 seconds. After sonication, sample protein concentrations were determined using a BCA assay kit (Pierce). Protein digestion was carried out by diluting 100 µg of protein from each sample with 50 mM NH_4HCO_3 in 6 M urea solution to a final volume of 100 µL, adding 1.5 M tris pH 8.8 (6.6 µL) and 200 mM tris (2-carboxyethyl)phosphine hydrochloride (2.5 µL) and vortexing samples. Samples were maintained at a basic pH > 7 by titrating with sodium hydroxide (5N). After incubating samples for one hour at 37°C, 20 µL of 200 mM iodoacetamide was added, samples were vortexed then incubated for one hour at room temperature in the dark. Next, 20 µL of 200 mM diothiothreitol was added, samples were vortexed, and incubated for one hour at room temperature. Then, 1.65 µL LysC (1:30 enzyme:protein ratio) was added to each sample, samples were vortexed, and incubated for one hour at room temperature. Finally, 800 µL 25 mM NH_4HCO_3, 200 µL HPLC grade methanol and 3.3 uL Trypsin (1:30 enzyme:protein ratio) were added to each sample, samples were vortexed, and incubated overnight at room temperature. Samples were evaporated using a centrifugal evaporator at 4°C to near dryness and stored at -80°C. Desalting of samples was done using Macrospin columns (sample capacity 0.03-300 ug; The Nest Group, Southborough, MA) following the manufacturer's instructions. Dried peptides were reconstituted in 100 µL 3% acetonitrile + 0.1% formic acid and stored at -80°C.

Mass Spectrometry

Data-dependent acquisition was performed on an Orbitrap Fusion Lumos Mass Spectrometer (Thermo Scientific) at the University of Washington Proteomics Resource to assess the effect of

temperature on proteomic profiles throughout larval development. Technical duplicates for each sample were processed by liquid chromatography coupled to tandem mass spectrometry (LC−MS/MS). Briefly, the analytical column (20 cm long) was packed in house with C18 beads (Dr. Maisch HPLC, Germany, 0.3 µm) with a flow rate of 0.3 µL/min. Chromatography was carried out with an increasing ratio of acetonitrile + 0.1% formic acid (solvent A):water + 0.1% formic acid (solvent B). The solvent gradient was 5-95% solvent A over 70 min. Quality-control standards (Pierce Peptide Retention Time Calibration mixture (PRTC) + bovine serum albumin (BSA)) were analyzed throughout the experiment to ensure consistency of peptide detection and elution times.

Protein identification and quantification

Mass spectrometer raw files (PRIDE Accession no. PXD013262) were converted to .mzXML format and were searched against a protein sequence database that contained the *C. gigas* proteome (downloaded from http://gigaton.sigenae.org (Riviere et al. 2015)) and common contaminants (downloaded from the crapOME (Mellacheruvu et al. 2013)) using Comet v. 2016.01 rev.2 (Eng et al. 2013). The Trans Proteomic Pipeline (Deutsch et al. 2010) was then used to calculate statistics associated with peptide-to-protein matches with a peptide probability *p*-value threshold of 0.9. Next, Abacus (Fermin et al. 2011) was used to correlate protein inferences across samples and obtain a single protein identification for each peptide. From the Abacus output file, the adjusted normalized spectral abundance factor (NSAF) values (spectral abundance normalized to protein sequence length) were used to compare technical duplicates and biological samples in a principal component analysis (PCA). For the PCA, NSAF values were log2 transformed after converting zero values to 0.1 (1/8 of the lowest NSAF value). NSAF values from technical replicates were averaged for each protein in all downstream analyses.

Preliminary principal component analysis

For a preliminary assessment of the overall variability of proteomes, PCA was run on log2 transformed NSAF values for all samples where NSAF values of zero were converted to 0.1 (1/8 of the lowest NSAF value) prior to log transforming. To identify proteins that most contribute to PC1 and PC2 variation, PC1 and PC2 protein loadings values were ordered and plotted by greatest magnitude loadings value (**Supplemental Figure 1**). For each loadings plot, a thresholded was placed at the point of diminishing returns, which for PC1 was a loadings value greater than 0.0236 or less than -0.02355, and for PC2 was a loadings value greater than 0.0245 or less than -0.0262 (**Supplemental Figure 2**). Proteins with a loadings value magnitude greater than or equal to the thresholds were considered proteins most contributing to variation accounting for temperature differences between samples from 21 and 27 dpf.

ANOVA-simultaneous component analysis

ANOVA-simultaneous component analysis (ASCA) from the R package MetStat (Dorscheidt 2013) was used to evaluate the effect of time, temperature, and their interaction on protein abundance using the log2 transformed average NSAF values for all samples. To quantitatively validate the significance of effects estimated by ASCA, a permutation test was performed that randomly reassigned group labels and recalculated the ASCA sum of squares 10,000 times (Zwanenburg et al. 2011). To identify proteins influenced by time, PC1 and PC2 loadings values of the ASCA-generated PCA for the time factor were ordered by decreasing magnitude and plotted. For each plot a loadings value threshold was placed at the point of diminishing returns, which for both PC1 and PC2 was ≥ 0.035 or ≤ -0.035 (**Supplemental Figure 3A-D**). To identify proteins influenced by temperature, PC1 loadings values of the ASCA-generated PCA for the temperature factor were ordered by decreasing mag plotted and a threshold was placed at the point of diminishing returns, which was ≥ 0.03 or ≤ -0.025 (**Supplemental Figure 3E-F**).

Cluster analysis

Hierarchical clustering was performed on temperature-influenced (identified by PCA or ASCA) and time-influenced proteins (identified by ASCA only) using the complete linkage clustering algorithm and Peasrson correlation-based distances. Dendrograms generated were cut at the height of 1 for proteins identified as temperature-influenced by PCA, 1.8 for time-influenced proteins identified by ASCA, and 1.5 for temperature-influenced proteins identified by ASCA to define clades within each group of proteins. Heatmaps of temperature- and time- influenced proteins with clades shown as a colored sidebar were generated using the R package Heatmap3 (Zhao et al. 2014) and protein abundance plots were generated using the R package ggplot2 (Wickham 2016).

Functional enrichment

To explore the biological processes related to proteins influenced by time and temperature, we performed gene ontology (GO) enrichment analysis on the proteins within each clade assigned by the aforementioned cluster analysis. First, to retrieve GO annotations protein sequences from the *C. gigas* proteome (downloaded from http://gigaton.sigenae.org (Riviere et al. 2015)) were queried against the UniProt protein database (UniProt release 2019_01 (The UniProt Consortium 2019)), a comprehensive reference set of protein sequences and functional information including GO annotations from thousands of species using BLASTp (Altschul et al. 1990). The rationale behind using a multi-species reference set as opposed to a species-specific reference set was to obtain functional information for as many proteins as possible where many *C.gigas* proteins lack annotation and homologs in other species may have annotations. The alignment with the lowest e-value was kept for each protein sequence, and alignments were filtered further for those with an e-value of less than or equal to 1×10^{-10} to keep only high confidence alignments. GO annotations from the Uniprot alignments were used for GO enrichment analysis. A Fisher test was performed with TopGO (Alexa A 2019) using default settings on proteins from

each clade defined by methods described above, using all detected proteins across all samples with GO annotations in the Uniprot alignments as the background set. GO terms with $P < 0.05$ and occuring ≥ 5 times in the background set were considered significant (Li et al. 2018). Correction for multiple testing was not applied on the resulting *P* values because the tests were not considered to be independent (Alexa et al. 2006). Significant GO terms were converted to GO Slim terms using the R package GSEAbase (Martin Morgan, Seth Falcon, and Robert Gentleman 2018), and heatmaps were generated using the heatmap.2 function in the R package gplots (Gregory R. Warnes, Ben Bolker, Lodewijk Bonebakker, Robert Gentleman, Wolfgang Huber Andy Liaw, Thomas Lumley, Martin Maechler, Arni Magnusson, Steffen Moeller, Marc Schwartz and Bill Venables 2019)**.**

Comparison to published datasets

Proteins influenced by time and temperature were compared to genes previously identified in other *C.gigas* proteomics studies exploring thermal stress on pediveliger stage (Dineshram et al. 2016) and an *in silico* transcriptomic study of larval settlement (Foulon et al. 2019) using their Uniprot identifiers. Because the Uniprot identifiers in these published datasets were from only the *C.gigas* species, *C. gigas* Uniprot identifiers were retrieved for temperature- and time-influenced proteins by aligning their protein sequences from the *C. gigas* proteome (downloaded from http://gigaton.sigenae.org (Riviere et al. 2015)) to the species-specific *C.gigas* reference proteome from Uniprot database (‘UP000005408_29159’) using BLASTp, keeping only the alignment with the lowest e-value for each protein sequence. Alignments were filtered for those with an e-value of less than or equal to 1×10^{-10} to keep only high confidence alignments. For temperature-influenced proteins that previously were identified and showed increased abundance in pediveliger proteomes arising from various heat stress conditions (Dineshram et al. 2016), functional information was retrieved from querying the Uniprot

knowledgebase (The UniProt Consortium 2019) with their Uniprot identifiers using the Retieve/ID mapping tool.

DATA ACCESS

Mass spectrometry proteomics data (.raw, .pepxml, and .mzXML files) have been deposited to the ProteomeXchange Consortium via the PRIDE (PubMed ID: 30395289) partner repository with the dataset identifier PXD013262. Supplemental files, additional supporting materials, and code is available at 10.6084/m9.figshare.12436598.

DISCLOSURE DECLARATION

The authors declare that they have no competing interests.

ACKNOWLEDGMENTS

We thank the Taylor Shellfish Hatchery for providing the animals, water treatment, rearing systems, and husbandry. We also thank the current and former members of the Roberts lab at the University of Washington as well as the University of Washington's Proteomics Resource (UWPR95794). This material is based upon work supported by the Washington Sea Grant award NA140AR4170078; project R/SFA-8.

AUTHOR CONTRIBUTIONS

S.B.R., B.V., and B.E. conceived the project. S.B.R., B.V., and B.E. advised research. R.E. and E.B.T.S. performed experiments. R.E. and S.B.R. performed proteomics analysis. S.A.T. performed statistical analyses with help from K.R.M. S.A.T. performed functional analyses. S.A.T. prepared the manuscript with edits from S.B.R., B.V., K.R.M., and E.B.T.S.

REFERENCES

Alexa A, Rahnenführer J, Lengauer T. 2006. Improved scoring of functional groups from gene expression data by decorrelating GO graph structure. *Bioinformatics* **22**: 1600–1607. http://dx.doi.org/10.1093/bioinformatics/btl140.

Alexa A RJ. 2019. *topGO: Enrichment Analysis for Gene Ontology*. https://bioconductor.org/packages/release/bioc/html/topGO.html.

Altschul SF, Gish W, Miller W, Myers EW, Lipman DJ. 1990. Basic local alignment search tool. *J Mol Biol* **215**: 403–410. http://dx.doi.org/10.1016/S0022-2836 (05)80360-2.

Assinder SJ, Stanton J-AL, Prasad PD. 2009. Transgelin: an actin-binding protein and tumour suppressor. *Int J Biochem Cell Biol* **41**: 482–486. http://dx.doi.org/10.1016/j.biocel.2008.02.011.

Baker SM, Mann R. 1994. Description of metamorphic phases in the oyster *Crassostrea virginica* and effects of hypoxia on metamorphosis. *Marine Ecology Progress Series* **104**: 91–99. http://dx.doi.org/10.3354/meps104091.

Casas-Vila N, Bluhm A, Sayols S, Dinges N, Dejung M, Altenhein T, Kappei D, Altenhein B, Roignant J-Y, Butter F. 2017. The developmental proteome of *Drosophila melanogaster*. *Genome Res* **27**: 1273–1285. http://dx.doi.org/10.1101/gr.213694.116.

Coon SL, Fitt WK, Bonar DB. 1990. Competence and delay of metamorphosis in the Pacific oyster *Crassostrea gigas*. *Marine Biology* **106**: 379–387. http://dx.doi.org/10.1007/bf01344316.

Crandall G, Elliot R, Euladiene B, Vadopalas B, Timmins-Schiffman EB, & Roberts SB. Proteomic response of early juvenile Pacific oysters to temperature. *Unpublished*.

Cunha SR, Bhasin N, Mohler PJ. 2007. Targeting and stability of Na/Ca exchanger 1 in cardiomyocytes requires direct interaction with the membrane adaptor ankyrin-B. *J Biol Chem* **282**: 4875–4883. http://dx.doi.org/10.1074/jbc.M607096200.

Deutsch EW, Mendoza L, Shteynberg D, Farrah T, Lam H, Tasman N, Sun Z, Nilsson E, Pratt B, Prazen B, et al. 2010. A guided tour of the Trans-Proteomic Pipeline. *Proteomics* **10**: 1150–1159. http://dx.doi.org/10.1002/pmic.200900375.

Dineshram R, Chandramouli K, Ko GWK, Zhang H, Qian P-Y, Ravasi T, Thiyagarajan V. 2016. Quantitative analysis of oyster larval proteome provides new insights into the effects of multiple climate change stressors. *Glob Chang Biol* **22**: 2054–2068. http://dx.doi.org/10.1111/gcb.13249.

Dorscheidt T. 2013. MetStaT: Statistical metabolomics tools. https://CRAN.R-project.org/package=MetStaT.

Eng JK, Jahan TA, Hoopmann MR. 2013. Comet: an open-source MS/MS sequence database search tool. *Proteomics* **13**: 22–24. http://dx.doi.org/10.1002/pmic.201200439.

Estes RM, Friedman CS, Elston RA, Herwig RP. 2004. Pathogenicity testing of shellfish hatchery bacterial isolates on Pacific oyster *Crassostrea gigas* larvae. *Dis Aquat Organ* **58**: 223–230.

http://dx.doi.org/10.3354/dao058223.

Fermin D, Basrur V, Yocum AK, Nesvizhskii AI. 2011. Abacus: a computational tool for extracting and pre-processing spectral count data for label-free quantitative proteomic analysis. *Proteomics* **11**: 1340–1345. http://dx.doi.org/10.1002/pmic.201000650.

Filgueira R, Brown MS, Comeau LA, Grant J. 2015. Predicting the timing of the pediveliger stage of *Mytilus edulis* based on ocean temperature. *Journal of Molluscan Studies* **81**: 269–273. http://dx.doi.org/10.1093/mollus/eyu093.

Foulon V, Boudry P, Artigaud S, Guérard F, Hellio C. 2019. In Silico Analysis of Pacific Oyster (*Crassostrea gigas*) Transcriptome over Developmental Stages Reveals Candidate Genes for Larval Settlement. *Int J Mol Sci* **20**. http://dx.doi.org/10.3390/ijms20010197.

Genard B, Miner P, Nicolas J-L, Moraga D, Boudry P, Pernet F, Tremblay R. 2013. Integrative Study of Physiological Changes Associated with Bacterial Infection in Pacific Oyster Larvae. *PLoS ONE* **8**: e64534. http://dx.doi.org/10.1371/journal.pone.0064534.

Ginger KWK, Vera CBS, R D, Dennis CKS, Adela LJ, Yu Z, Thiyagarajan V. 2013. Larval and post-larval stages of Pacific oyster (*Crassostrea gigas*) are resistant to elevated CO2. *PLoS One* **8**: e64147. http://dx.doi.org/10.1371/journal.pone.0064147.

Gregory R. Warnes, Ben Bolker, Lodewijk Bonebakker, Robert Gentleman, Wolfgang Huber Andy Liaw, Thomas Lumley, Martin Maechler, Arni Magnusson, Steffen Moeller, Marc Schwartz and Bill Venables. 2019. *gplots: Various R Programming Tools for Plotting Data*. https://CRAN.R-project.org/package=gplots.

Griffin NM, Yu J, Long F, Oh P, Shore S, Li Y, Koziol JA, Schnitzer JE. 2010. Label-free, normalized quantification of complex mass spectrometry data for proteomic analysis. *Nat Biotechnol* **28**: 83–89. http://dx.doi.org/10.1038/nbt.1592.

Grissa D, Pétéra M, Brandolini M, Napoli A, Comte B, Pujos-Guillot E. 2016. Feature Selection Methods for Early Predictive Biomarker Discovery Using Untargeted Metabolomic Data. *Front Mol Biosci* **3**: 30. http://dx.doi.org/10.3389/fmolb.2016.00030.

Helm MM, Bourne N. 2004. *Hatchery Culture of Bivalves: A Practical Manual*. Food & Agriculture Org https://books.google.com/books/about/Hatchery_Culture_of_Bivalves.html?hl=&id=hFUbAQAAIAAJ.

Helm MM, Millican PF. 1977. Experiments in the hatchery rearing of Pacific oyster larvae (*Crassostrea gigas* Thunberg). *Aquaculture* **11**: 1–12. http://dx.doi.org/10.1016/0044-8486 (77)90149-1.

His E, Robert R, Dinet A. 1989. Combined effects of temperature and salinity on fed and starved larvae of the mediterranean mussel *Mytilus galloprovincialis* and the Japanese oyster *Crassostrea gigas*. *Marine Biology* **100**: 455–463. http://dx.doi.org/10.1007/bf00394822.

Holmgren A, Bouhy D, De Winter V, Asselbergh B, Timmermans J-P, Irobi J, Timmerman V. 2013. Charcot-Marie-Tooth causing HSPB1 mutations increase Cdk5-mediated phosphorylation of neurofilaments. *Acta Neuropathol* **126**: 93–108. http://dx.doi.org/10.1007/s00401-013-1133-6.

Huan P, Wang H, Dong B, Liu B. 2012. Identification of differentially expressed proteins involved in the early larval development of the Pacific oyster *Crassostrea gigas*. *J Proteomics* **75**: 3855–3865. http://dx.doi.org/10.1016/j.jprot.2012.04.051.

Huan P, Wang H, Liu B. 2015. A Label-Free Proteomic Analysis on Competent Larvae and Juveniles of the Pacific Oyster *Crassostrea gigas*. *PLoS One* **10**: e0135008. http://dx.doi.org/10.1371/journal.pone.0135008.

Humphries S. 2013. A physical explanation of the temperature dependence of physiological processes mediated by cilia and flagella. *Proc Natl Acad Sci U S A* **110**: 14693–14698. http://dx.doi.org/10.1073/pnas.1300891110.

Joyce A, Vogeler S. 2018. Molluscan bivalve settlement and metamorphosis: Neuroendocrine inducers and morphogenetic responses. *Aquaculture* **487**: 64–82. http://dx.doi.org/10.1016/j.aquaculture.2018.01.002.

Kobayashi M, Hofmann EE, Powell EN, Klinck JM, Kusaka K. 1997. A population dynamics model for the Japanese oyster, *Crassostrea gigas*. *Aquaculture* **149**: 285–321. http://dx.doi.org/10.1016/s0044-8486 (96)01456-1.

Korringa P. 1976. *Farming the Cupped Oysters of the Genus Crassostrea: A Multidisciplinary Treatise*. Elsevier Science Limited https://books.google.com/books/about/Farming_the_Cupped_Oysters_of_the_Genus.html?hl=&id=jVYYAQAAIAAJ.

Kostenko S, Johannessen M, Moens U. 2009. PKA-induced F-actin rearrangement requires phosphorylation of Hsp27 by the MAPKAP kinase MK5. *Cell Signal* **21**: 712–718. http://dx.doi.org/10.1016/j.cellsig.2009.01.009.

Li Y, Liew YJ, Cui G, Cziesielski MJ, Zahran N, Michell CT, Voolstra CR, Aranda M. 2018. DNA methylation regulates transcriptional homeostasis of algal endosymbiosis in the coral model Aiptasia. *Sci Adv* **4**: eaat2142. http://dx.doi.org/10.1126/sciadv.aat2142.

Martin Morgan, Seth Falcon, and Robert Gentleman. 2018. GSEABase: Gene set enrichment data structures and methods. https://bioconductor.org/packages/release/bioc/html/GSEABase.html.

Masood M, Raftos DA, Nair SV. 2016. Two Oyster Species That Show Differential Susceptibility to Virus Infection Also Show Differential Proteomic Responses to Generic dsRNA. *J Proteome Res* **15**: 1735–1746. http://dx.doi.org/10.1021/acs.jproteome.5b00615.

Matsui TS, Ishikawa A, Deguchi S. 2018. Transgelin-1 (SM22α) interacts with actin stress fibers and podosomes in smooth muscle cells without using its actin binding site. *Biochem Biophys Res Commun* **505**: 879–884. http://dx.doi.org/10.1016/j.bbrc.2018.09.176.

Meistertzheim A-L, Tanguy A, Moraga D, Thébault M-T. 2007. Identification of differentially expressed genes of the Pacific oyster *Crassostrea gigas* exposed to prolonged thermal stress. *FEBS J* **274**: 6392–6402. http://dx.doi.org/10.1111/j.1742-4658.2007.06156.x.

Mellacheruvu D, Wright Z, Couzens AL, Lambert J-P, St-Denis NA, Li T, Miteva YV, Hauri S, Sardiu ME, Low TY, et al. 2013. The CRAPome: a contaminant repository for affinity purification-mass

spectrometry data. *Nat Methods* **10**: 730–736. http://dx.doi.org/10.1038/nmeth.2557.

Mohler PJ, Schott J-J, Gramolini AO, Dilly KW, Guatimosim S, duBell WH, Song L-S, Haurogné K, Kyndt F, Ali ME, et al. 2003. Ankyrin-B mutation causes type 4 long-QT cardiac arrhythmia and sudden cardiac death. *Nature* **421**: 634–639. http://dx.doi.org/10.1038/nature01335.

O'Connor MI, Bruno JF, Gaines SD, Halpern BS, Lester SE, Kinlan BP, Weiss JM. 2007. Temperature control of larval dispersal and the implications for marine ecology, evolution, and conservation. *Proceedings of the National Academy of Sciences* **104**: 1266–1271. http://dx.doi.org/10.1073/pnas.0603422104.

Plough LV. 2018. Fine-scale temporal analysis of genotype-dependent mortality at settlement in the Pacific oyster *Crassostrea gigas*. *Journal of Experimental Marine Biology and Ecology* **501**: 90–98. https://doi.org/10.1016/j.jembe.2018.01.006.

Quayle DB. 1988. *Pacific oyster culture in British Columbia*. Dept. of Fisheries and Oceans.

Renault T, Novoa B. 2004. Viruses infecting bivalve molluscs. *Aquatic Living Resources* **17**: 397–409. http://dx.doi.org/10.1051/alr:2004049.

Rico-Villa B, Pouvreau S, Robert R. 2009. Influence of food density and temperature on ingestion, growth and settlement of Pacific oyster larvae, *Crassostrea gigas*. *Aquaculture* **287**: 395–401. http://dx.doi.org/10.1016/j.aquaculture.2008.10.054.

Riviere G, Klopp C, Ibouniyamine N, Huvet A, Boudry P, Favrel P. 2015. GigaTON: an extensive publicly searchable database providing a new reference transcriptome in the pacific oyster *Crassostrea gigas*. *BMC Bioinformatics* **16**: 401. http://dx.doi.org/10.1186/s12859-015-0833-4.

Smilde AK, Jansen JJ, Hoefsloot HCJ, R-J A, van der Greef J, Timmerman ME. 2005. ANOVA-simultaneous component analysis (ASCA): a new tool for analyzing designed metabolomics data. *Bioinformatics* **21**: 3043–3048. http://dx.doi.org/10.1093/bioinformatics/bti476.

Solomon S, Xu Y, Wang B, David MD, Schubert P, Kennedy D, Schrader JW. 2007. Distinct structural features of caprin-1 mediate its interaction with G3BP-1 and its induction of phosphorylation of eukaryotic translation initiation factor 2alpha, entry to cytoplasmic stress granules, and selective interaction with a subset of mRNAs. *Mol Cell Biol* **27**: 2324–2342. http://dx.doi.org/10.1128/MCB.02300-06.

The UniProt Consortium. 2019. UniProt: a worldwide hub of protein knowledge. *Nucleic Acids Research* **47**: D506–D515. http://dx.doi.org/10.1093/nar/gky1049.

Thweatt R, Lumpkin CK Jr, Goldstein S. 1992. A novel gene encoding a smooth muscle protein is overexpressed in senescent human fibroblasts. *Biochem Biophys Res Commun* **187**: 1–7. http://dx.doi.org/10.1016/s0006-291x (05)81449-4.

Trigg SA, McElhany P, Maher M, Perez D, Busch DS, & Nichols KM. 2019. Uncovering mechanisms of global ocean change effects on the Dungeness crab (*Cancer magister*) through metabolomics analysis. *bioRxiv*. http://dx.doi.org/10.1101/574798.

Ushijima B, Richards GP, Watson MA, Schubiger CB, Häse CC. 2018. Factors affecting infection of

corals and larval oysters by *Vibrio coralliilyticus*. *PLoS One* **13**: e0199475. http://dx.doi.org/10.1371/journal.pone.0199475.

Wickham H. 2016. *ggplot2: Elegant Graphics for Data Analysis*. Springer-Verlag New York.

Yu H, Zhao X, Li Q. 2016. Genome-wide identification and characterization of long intergenic noncoding RNAs and their potential association with larval development in the Pacific oyster. *Sci Rep* **6**: 20796. http://dx.doi.org/10.1038/srep20796.

Zhao S, Guo Y, Sheng Q, Shyr Y. 2014. Heatmap3: an improved heatmap package with more powerful and convenient features. *BMC Bioinformatics* **15**: P16. http://dx.doi.org/10.1186/1471-2105-15-s10-p16.

Zwanenburg G, Hoefsloot HCJ, Westerhuis JA, Jansen JJ, Smilde AK. 2011. ANOVA-principal component analysis and ANOVA-simultaneous component analysis: a comparison. *Journal of Chemometrics* **25**: 561–567. http://dx.doi.org/10.1002/cem.1400.